5.0 Introduction to MODIS Cloud Products

Bryan A. Baum[1], Steven Platnick[2]

[1]Atmospheric Sciences, NASA Langley Research Center, Hampton, VA
[2]Laboratory for Atmospheres, NASA Goddard Space Flight Center, Greenbelt, MD 20771

5.1 Introduction

The Earth's radiative energy balance and hydrological cycle are fundamentally coupled with the distribution and properties of clouds. Therefore, the ability to remotely infer cloud properties and their variation in space and time is crucial for establishing climatologies as a reference for validation of present-day climate models and in assessing future climate change. Remote cloud observations also provide data sets useful for testing and improving cloud model physics, and for assimilation into numerical weather prediction models.

The MODerate Resolution Imaging Spectroradiometer (MODIS) imagers on the Terra and Aqua Earth Observing System (EOS) platforms provide the capability for globally retrieving these properties using passive solar reflectance and infrared techniques. In addition to providing measurements similar to those offered on a suite of historical operational weather platforms such as the Advanced Very High Resolution Radiometer (AVHRR), the High-resolution Infrared Radiation Sounder (HIRS), and the Geostationary Operational Environmental Satellite (GOES), MODIS provides additional spectral and/or spatial resolution in key atmospheric bands, along with onboard calibration, to expand the capability for global cloud property retrievals.

The core MODIS operational cloud products include cloud top pressure, thermodynamic phase, optical thickness, particle size, and water path, and are derived globally at spatial resolutions of either 1- or 5-km (referred to as Level-2 or pixel-level products). In addition, the MODIS atmosphere team (collectively providing cloud, aerosol, and clear sky

products) produces a combined gridded product (referred to as Level-3) aggregated to a 1° equal-angle grid, available for daily, eight-day, and monthly time periods. The wealth of information available from these products provides critical information for climate studies as well as the continuation and improved understanding of existing satellite-based cloud climatologies derived from heritage instruments.

This chapter provides an overview of the MODIS Level-2 and -3 operational cloud products. All products described in this chapter are available from the NASA Goddard Earth Sciences Distributed Active Archive Center (GES DAAC). However, the MODIS instrument has direct broadcast capability on both the Terra and Aqua platforms. Ground stations that obtain the MODIS data as the spacecraft passes within range, can obtain free software to generate the operational cloud products in near-real time. New applications using these near real-time cloud products are being explored by a number of users.

5.2 MODIS Instrument and Calibration

MODIS is a 36-band whiskbroom scanning radiometer currently flying on the NASA Terra and Aqua platforms. Terra was launched in December, 1999, and is in a (daytime) descending orbit with an equatorial crossing of 1030 local solar time. Aqua, launched in May 2002, is in an ascending orbit with a 1330 local crossing time. The instrument is comprised of four focal planes covering the spectral range 0.42–14.24 μm, with each spectral band defined by an interference filter. Spatial resolution for nadir views varies from 250 m to 1 km, depending on the spectral band. MODIS has several onboard instruments for in-orbit radiometric and spectral characterization. A solar diffuser panel is used for reflectance calibration for bands with wavelengths from 0.45 through 2.1 μm, and an accompanying diffuser stability monitor is used to assess the stability of the diffuser at wavelengths up to 1 μm. Thermal spectral bands are calibrated with an onboard blackbody.

This chapter will describe briefly the comprehensive set of remote sensing algorithms used by the MODIS atmosphere science Team to infer cloud properties. The description begins with pixel-level geolocated and calibrated (radiance and/or reflectance-based) data known as Level-1B (L1B). Pixel-level cloud properties, at either 1-km or 5-km resolution, are based on the L1B data and ancillary data streams discussed later in this chapter. The pixel-level cloud product is referred to as Level-2, and is typically stored for a 5-minute granule of data. Based on the Level-2

product, a set of global gridded statistics products are developed and are labeled as Level-3.

The cloud property retrieval algorithms depend critically on accurate characterization and calibration of the L1B radiance and reflectance data from both Terra and Aqua MODIS imagers. Considerable time and attention have been given in the post-launch era to understanding and mitigating performance issues (through characterization) such as longwave infrared (IR) band cross-talk, scan mirror reflectance variation with scan angle, thermal leakage into reflective band measurements, and detector striping. Part of this effort has been to verify the radiometric integrity of MODIS measurements (Moeller et al. 2003). As performance issues have been addressed, adjustments have been incorporated into the MODIS L1B production code for use in the various processing streams (known as a *Collection*) of MODIS L1B and Level 2 products. Each collection includes reprocessing of historical MODIS data and forward processing of the ongoing measurements, until the beginning of the next collection. Each collection uses the best available post-launch instrument characterization, as well as science product algorithm improvements such as improved treatment of surface radiative characteristics (spectral albedo, emissivity, and skin temperature), mitigation of day-night science product biases, and improved production code efficiency.

For example, pre-launch testing of the MODIS proto-flight model (PFM) on Terra revealed a light leak from the infrared window (band 31, 11 μm) into bands 32-36 (wavelengths ranging from 12 to 14.3 μm). To complicate matters, the leak included both spatial and spectral components. The radiometric impact for typical radiances in these bands ranged from less than 1% in band 32 to more than 10% in band 36. These impacts are near or exceed the MODIS radiometric accuracy specification of 0.5% (band 32) and 1% (bands 33-36) at typical scene temperatures. A simple linear correction algorithm was developed to reduce the contamination in these bands.

As another example, the Terra MODIS scan mirror Response Versus Scan angle (RVS) characterization was not measured at the system level in pre-launch tests. Shortly after launch, it was found that an unexpectedly large asymmetry was present in the MODIS longwave infrared (LWIR) bands. In other words, there was a difference in the radiances from one side of the scan to the other, and this in turn led to systematic biases in several cloud products as a function of scan. A Terra deep space maneuver was performed in 2003; the resulting high quality RVS characterization was applied to the operational L1B processing algorithm and effectively removed the RVS asymmetry in the LWIR bands.

With careful and continual evaluation of the instrument and cloud products, production runs are of much higher quality than earlier versions. Up-to-date information on Terra and Aqua algorithm versions and reprocessing efforts are given on the MODIS atmosphere group web site (http://modis-atmos.gsfc.nasa.gov/products_calendar.html).

5.3 Level – 2 Cloud Products

The MODIS cloud products are generated on a granule basis; a granule is 5 minutes of data and typically consists of 2030 along-track pixels. The suite of operational cloud products (Platnick et al. 2003) begins with cloud detection or masking, i.e., deciding whether or not a cloud is present. Infrared techniques are employed to estimate cloud top pressure, effective cloud amount (product of cloud fraction and cloud emittance), and cloud thermodynamic phase. In daytime data, cloud optical thickness and effective particle size are provided using solar reflectance techniques. A cirrus reflectance retrieval is provided separately. The following sections provide background on the methodology used to infer these various parameters. With the exception of the cloud mask, all cloud products are archived in a single Hierarchical Data Format (HDF) file with the product designation MOD06; the cloud mask product is in MOD35.

5.3.1 Cloud Masking

The focus of the product is to indicate a level of confidence as to whether the satellite has an unobstructed field-of-view (FOV) to a pixel's location on the surface. The MODIS cloud mask product serves as the primary ancillary input to the other cloud algorithms (Ackerman et al., 1998). In addition to the potential for obstruction in the line of sight due to clouds, heavy aerosols (e.g., smoke) and dust will also act to decrease the likelihood of finding clear-sky conditions. The product provides more information than a simple yes/no decision; there are 48 bits of output per 1-km pixel that includes information on sets of multispectral test results, the processing path, and limited ancillary information such as a land/ocean tag. The first eight bits provide a summary sufficient for most applications. Additionally, the first two bits simply offer information in four categories: *confident clear, probably clear, uncertain/probably cloudy*, and *cloudy*.

The algorithm uses a variety of multispectral tests involving combinations of up to 19 spectral bands. The use of these bands changes somewhat as calibration issues are mitigated. Different sets of tests are

applied depending on the surface (land, water, snow/ice, desert, and coast) and solar illumination (day/twilight/night). In addition to the multispectral tests, a textural test is applied over ocean to improve the detection of dust.

Several ancillary data sets are used in the cloud detection process. Surface snow and ice data are provided at 25 km resolution by the Near Real-Time Ice and Snow Extent (NISE) product from the National Snow and Ice Data Center. The NCEP Reynolds blended SST product (Reynolds and Smith, 1994) has been implemented to improve the product at nighttime over oceans and in areas where there are strong temperature gradients such as in the vicinity of the Gulf Stream.

5.3.2 Cloud Thermodynamic Phase

There are currently three inferences of cloud phase found in the MOD06 cloud product: (1) a bispectral IR algorithm stored as a separate Science Data Set (SDS), (2) a set of shortwave IR (SWIR) tests, and (3) a decision tree algorithm that includes cloud mask results as well as the IR and SWIR tests. The latter two phase retrievals are stored in the MODIS "Quality_Assurance_1km" output SDS and not as individual SDS's. The decision tree algorithm provides the phase used in the subsequent optical and microphysical retrieval. The current IR phase algorithm is at a 5 km spatial resolution, while the other two are at 1 km. This section will summarize the IR phase retrieval (Strabala et al. 1994; Baum et al. 2000b). Details on the SWIR and decision tree phase tests are beyond the scope of this chapter, but can be found in Platnick et al. (2003).

The IR phase retrieval provides four categories: *ice, water, mixed phase*, and *uncertain*. A "mixed phase" cloud is thought to consist of a mixture of ice and water particles. With the IR-based method, cloud phase is inferred from the brightness temperature difference (BTD) between the 8.5 and 11 μm brightness temperatures (BTD[8.5-11]) as well as the 11-μm brightness temperature. The physical basis for this approach stems from the observation that the imaginary component of the index of refraction differs for ice and water at these two wavelengths. The BTD[8.5-11] is affected by atmospheric water vapor absorption, surface emissivity, and cloud particle size (small particles scatter more radiation than large particles). Radiative transfer simulations show that for ice clouds, the BTD[8.5-11] values tend to be positive in sign, whereas for low-level water clouds, the BTD[8.5-11] values tend to be very negative. This simple bispectral IR technique is adequate for classifying the phase as either "ice" or "water" for about 80% of the cloudy pixels on a global basis. The most problematic areas are optically thin cirrus, multilayered

clouds (especially thin cirrus over lower-level water clouds), and single-layered clouds having cloud top temperatures between 233K and 273K (i.e., supercooled water or "mixed phase" clouds). Supercooled water or mixed-phase clouds tend to occur most frequently in the high latitude storm belts of both hemispheres.

To improve the inference of cloud phase during daytime, a decision tree algorithm is implemented during the processing step where cloud optical thickness and effective particle size is inferred (Platnick et al. 2003; King et al. 2004). The decision tree begins with the cloud mask results as well as the bispectral IR cloud phase results, and incorporates tests using reflectances obtained at a visible wavelength (e.g., 0.65 μm) and a shortwave-infrared (SWIR) wavelength (e.g., 1.64 μm or 2.15 μm). At wavelengths less than about 0.7 μm, clouds composed of either liquid or ice tend to absorb very little solar radiation. At the SWIR wavelength, the imaginary index of refraction values for both water and ice increase in comparison with those at the visible wavelength. However, the values for ice and water diverge from each other, with ice having a higher imaginary index of refraction than that of water. Even with these supplementary tests, mixed-phase clouds remain a challenge.

5.3.3 Cloud Top Pressure and Effective Cloud Amount

For the past several decades, a technique known as CO_2 slicing has been used to infer cloud-top pressure and effective cloud amount (the product of the cloud fraction and the cloud emittance) from radiances measured in spectral bands located within the broad 15-μm CO_2 absorption region. As the wavelength increases from 13.3 μm to 15 μm, the atmosphere becomes more opaque due to CO_2 absorption, thereby causing radiances obtained from these spectral bands to be sensitive to a different portion of the atmosphere. This technique has been applied to data from the High resolution Infrared Radiometer Sounder (HIRS; Wylie and Menzel 1999) as well as the Geostationary Operational Environmental Satellite (GOES) sounder (Menzel et al. 1992; Menzel and Purdom 1994). The field of view (FOV) size for HIRS at nadir is approximately 18 km and for GOES is 10 km. MODIS provides measurements at 1-km resolution and at four wavelengths located in the broad 15-μm CO_2 band, but cloud top properties are produced at 5-km spatial resolution.

The MODIS cloud pressure is converted to cloud temperature through the use of gridded meteorological products that provide temperature profiles at some nominal vertical resolution every 6 hours. The product used for this purpose is provided by the NCEP Global Data Assimilation

System (GDAS; Derber et al. 1991). It has been noticed that differences exist between measured and calculated (i.e., model derived) clear-sky radiances. Further discussion on an effort to mitigate this issue is presented in Section 5.5.4.

There are many benefits to the CO_2 slicing algorithm, foremost of which is its unique heritage and application to data spanning a record of more than 25 years. Cloud properties are derived similarly for both daytime and nighttime data as the IR method is independent of solar illumination. This approach is very useful for the analysis of midlevel to high-level clouds, and especially semi-transparent clouds such as cirrus. One constraint to the use of the 15-μm channels is that the cloud signal (change in radiance caused by the presence of cloud) becomes comparable to instrument noise for optically thin clouds and for clouds occurring in the lowest 3 km of the atmosphere. When low clouds are present, cloud top temperature is adjusted until agreement is achieved between model-calculated and observed 11-μm radiances; cloud top pressure is then estimated by matching the temperature to the GDAS profile.

Figure 5.1 shows a true color image of an Aqua scene from 20 November 2000 at 1710 UTC, encompassing north–central South America, specifically Trinidad, Venezuela, Guyana, Suriname, French Guiana, and Brazil. This true-color image is created by superimposing three bands: 0.65 μm (band 1 in red), 0.55 μm (band 4 in green), and 0.47 μm (band 3 in blue). Clouds are white but display a variety of textures and spatial scales. The land surfaces appear as green or brown depending on the amount of surface vegetation, while deep–ocean appears as dark blue. Shallow coastal waters are light blue or brown in appearance. Retrieved cloud-top pressures (Figure 5.2a) and temperatures (Figure 5.2b) are obtained at 5-km spatial resolution. From the range of cloud-top temperature, one gains a sense of the complexity inherent in such retrievals. Not only do the cloud properties change over short horizontal distances, but often high- and low-level clouds co-exist.

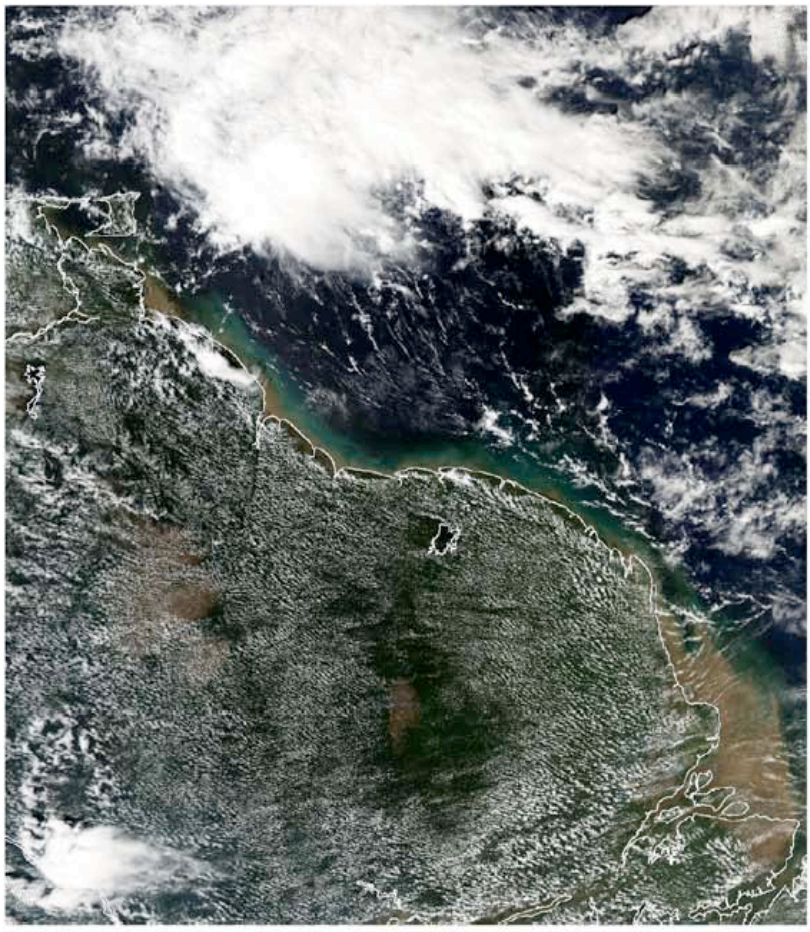

Fig. 5.1. True color image of an Aqua scene from 20 November, 2000 at 1710 UTC, encompassing north central South America, specifically Trinidad, Venezuela, Guyana, Suriname, French Guiana, and Brazil. This true-color image is created by superimposing three bands: 0.65 μm (band 1 in red), 0.55 μm (band 4 in green), and 0.47 μm (band 3 in blue). Clouds are white but display a variety of textures and spatial scales. The land surfaces appear as green or brown depending on the amount of surface vegetation, while deep ocean appears as dark blue. Shallow coastal waters are light blue or brown in appearance

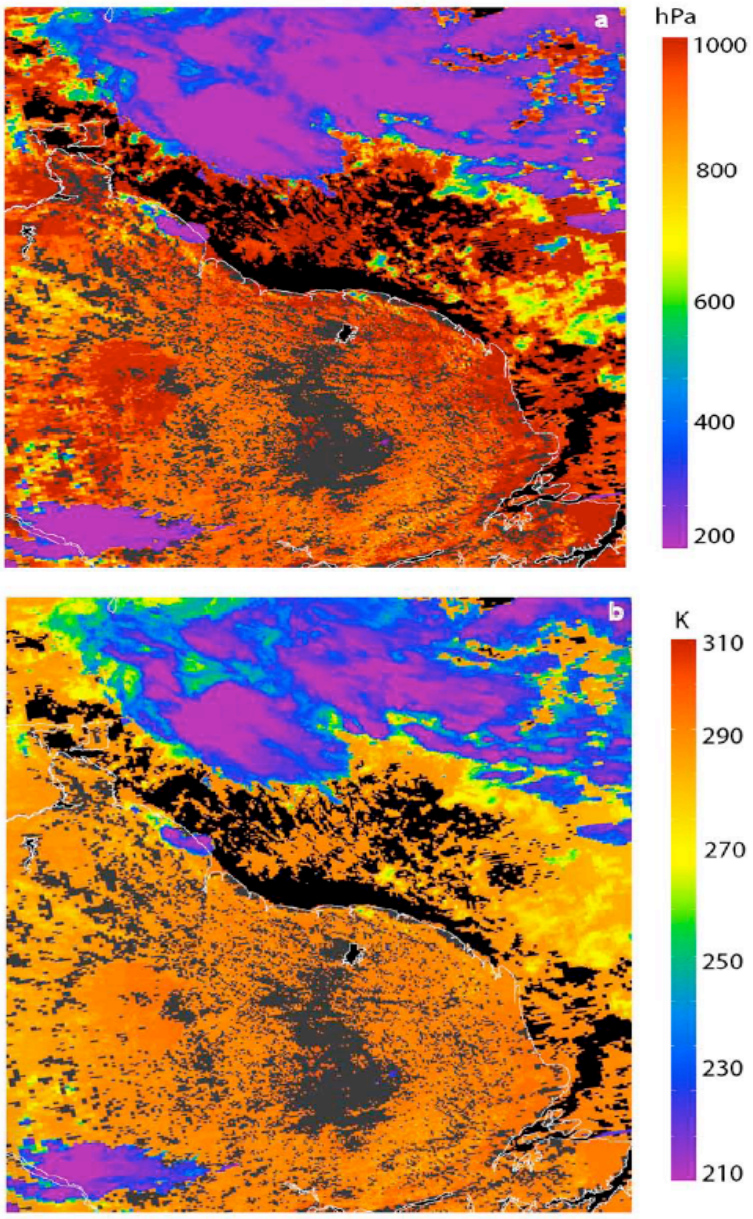

Fig. 5. 2. (a) Retrieved cloud-top pressure in hPa and (b) cloud-top temperature in Kelvin obtained at 5-km spatial resolution for the scene in Figure 5.1

5.3.4 Cloud Optical and Microphysical Properties

Cloud optical thickness is defined as the vertical integration of extinction over the cloud physical thickness. For water clouds composed of spherical particles, effective particle size is defined as the ratio of the third moment to the second moment of the particle size distribution. The definition of effective particle size for ice clouds is made more difficult because ice particles tend to be non-spherical. For ice clouds, the effective particle size is defined as being proportional to the ratio of the total volume to the projected area of the ice particles for a given size and habit distribution.

The simultaneous retrieval of optical thickness and effective particle size derived from cloud reflectance measurements in solar band atmospheric windows is well known. MODIS retrievals are performed using a band that is practically non-absorbing for bulk water/ice (0.65, 0.86, or 1.2 μm) combined with three longer wavelength bands where bulk water/ice has significant absorption (1.6, 2.1, and 3.7 μm). Three separate effective sizes are provided in MOD06 corresponding to each of these absorbing bands. The 3.7 μm band includes a significant thermal emission component in addition to the solar reflectance component. A proper accounting of the thermal emission must include consideration of cloud top temperature, emissivity (a function of cloud microphysics), and above-cloud atmospheric emission and transmittance. In addition, for clouds with optical thicknesses less than about 6, transmittance of surface emission through the cloud can be important. Because of these additional complexities, the 3.7-μm retrievals are thought to be of higher uncertainty than those from the other two bands. However, the 3.7-μm results are included in the MOD06 product because of this band's heritage on earlier satellite imagers such as the AVHRR.

The 2.1-μm band retrieval of effective particle size for water clouds is preferred to the 1.6-μm retrieval because of the increased absorption (the imaginary index of refraction is about an order of magnitude higher for water at 2.1 than at 1.6 μm). Additionally, more than half of the 1.6-μm detectors are inoperative on the Aqua platform, rendering the use of this band problematic. The 2.1-μm band retrieval of effective particle size is the default quantity used in Level-3 aggregations, which are discussed later in this chapter. MODIS is the first satellite imager to take measurements in each of these absorbing bands simultaneously.

The retrievals are based on library calculations of plane–parallel homogeneous clouds overlying a black surface in the absence of an atmosphere. Separate libraries have been built for water and ice clouds; currently no separate library exists for mixed phase clouds. The bulk scattering properties for the ice clouds are based on mixtures of hexagonal

plates, columns, bullet rosettes, and aggregates (Baum et al. 2000a; King et al. 2004) and a set of particle size distributions developed from midlatitude cirrus field campaigns.

When clouds are not opaque, reflected sunlight for overcast pixels can be significantly affected by the reflectivity of the underlying surface. Over land, the surface albedo is highly variable, both spectrally and with surface type. Over water, surface reflectance can increase significantly due to sun glint. Ice- and snow-covered surfaces are bright at a visible wavelength but dark in SWIR bands.

Realistic estimates of the surface reflectance beneath clouds, as well as corrections for atmospheric transmittance, are now employed on a pixel basis during operational processing. Towards this end, the MODIS operational surface spectral albedo/BRDF (bidirectional reflectance distribution function) product (MOD43) provides 16-day composites of clear-sky observations at 1-km spatial resolution for both BRDF and albedo. The spectral albedo product includes both solar illumination and diffuse sky values. All further references to surface albedo refer to the diffuse sky albedo since this is the quantity most relevant to cloud property retrievals. More specifically, diffuse sky is officially referred to as the "white sky albedo" in the MOD43 product, and means the albedo with lambertian incident intensity. These properties are provided for all the relevant MODIS solar bands (except at 3.7 μm). From a 16-day composite available at the time of the last major algorithm delivery, data are composited and aggregated by land cover type to determine the extent to which ecosystem was useful as a predictor of spectral albedo. The MODIS land cover product (MOD12) is used in this effort. Dispersions in spectral diffuse albedo were generally found to be less than 20% for any given ecosystem. With the ecosystem-based albedo aggregations in three separate latitude bands, a sinusoidal fit was made between the summer/winter extremes to replicate the seasonal cycle. An upcoming delivery will include spectral albedo composited from a year of MOD43 data, and is discussed further in Section 5.5.3. For operational processing, snow and ice cover is provided by the NISE product; when snow or ice is present, spectral albedos are provided from field measurements. Further details regarding the MODIS optical and microphysical retrieval algorithm are described in Platnick et al. (2003).

Figure 5.3 shows the retrieved optical thickness (Fig. 5.3a) and effective particle size (Fig. 5.3b) for ice and water clouds for the same scene shown in Figure 5.1. These results are obtained at 1-km spatial resolution in contrast to the cloud top pressure at 5-km resolution. Inherent in this image is the classification of cloud thermodynamic phase. Ice cloud optical

thickness and effective particle radius values are shown on a logarithmic scale in colors ranging from purple to green, while water cloud values are displayed in colors ranging from yellow to red.

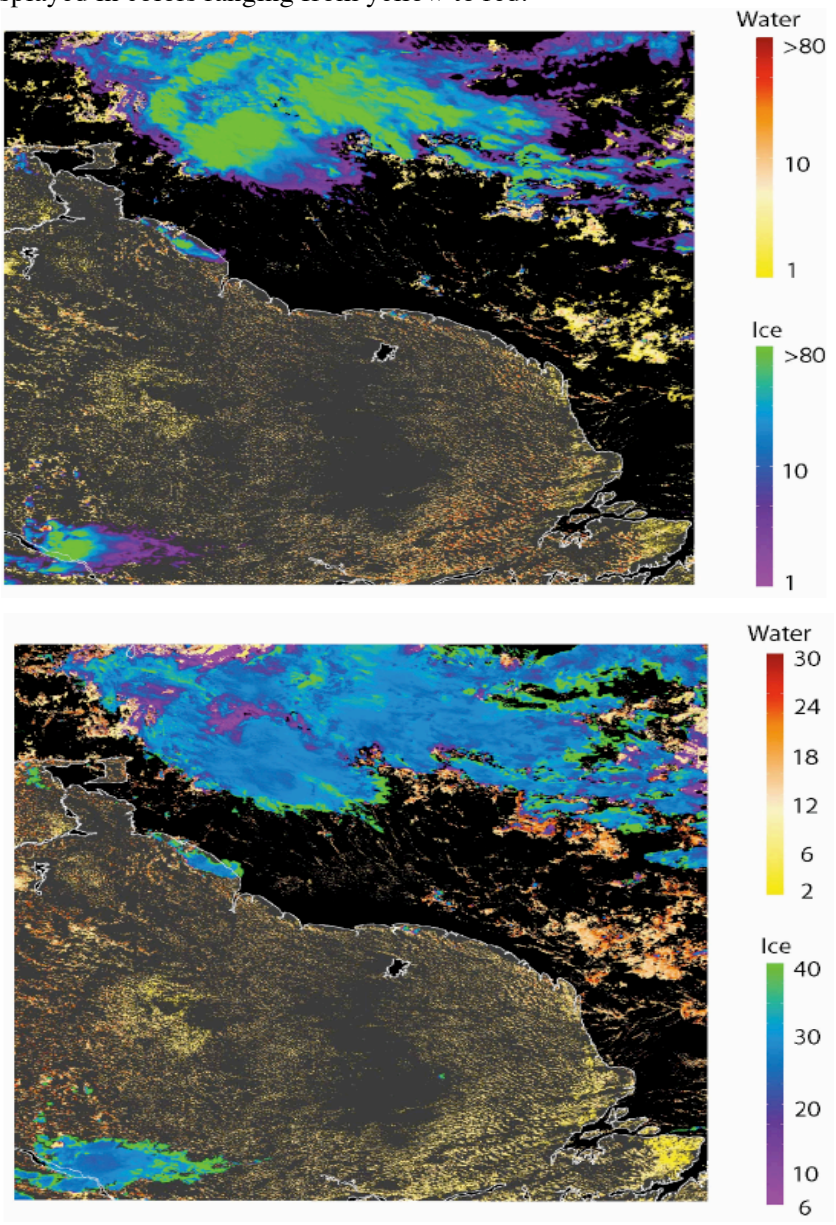

Fig. 5.3. (a) Retrieved cloud optical thickness and (b) effective particle size for both ice- and water-phase clouds at 1-km spatial resolution for the scene in Figure 5.1

Over land, note that the lower clouds are cellular, likely having sub-pixel scales that violate the plane–parallel assumption (i.e., homogeneous in the horizontal plane) used by both the optical and microphysical retrieval algorithm and the 11-μm cloud top temperature algorithm (used for low clouds). Partly cloudy pixels will fundamentally impact the cloud mask, cloud thermodynamic phase, and cloud height retrievals as well.

5.3.5 Cirrus Reflectance Algorithm

One type of ice cloud that is particularly difficult to quantify from satellite data is semitransparent cirrus due to its wide range of microphysical (e.g., particle size and shape), macrophysical (height and temperature), and optical properties (bulk scattering characteristics). The variation in these cirrus properties results in large spatial and temporal variability of optical thickness and emittance. MODIS has a unique spectral reflectance channel at 1.38-μm that is centered near a strong water vapor absorption band. The upwelling radiance is attenuated by the low-level water vapor so that there is little or no contribution by the radiation reflected by the surface and scattered by the low-level particulate atmospheric constituents (e.g., dust and aerosols). The reflectance measured at this wavelength is primarily from the presence of mid- to high-level clouds. Once the high-level cloud (cirrus) reflectance component is identified, the equivalent reflectance in the MODIS 0.65 μm band is inferred through an empirical technique. Further details may be found in Gao et al. (2002).

5.4 Global Gridded (Level – 3) Products

Once the Level-2 granule-level cloud products have been produced, spatial and temporal composites are aggregated to daily, eight-day, and monthly files. Statistics are sorted onto a *1° x 1°* equal-angle grid (row by column) containing *180 x 360* individual cells. The Level-3 atmosphere product, MOD08, is derived separately for Aqua and Terra. For the daily product, every Level-2 granule that overlaps any part of the data day, defined as being from 0000 to 2400 UTC, is included in the temporal compositing process. A granule that spans either 0000 UTC or 2400 UTC may be included in two consecutive MOD08 daily products. The eight-day product is derived from the daily Level-3 products summarized over eight consecutive days. The eight-day intervals are reset at the beginning of each year similarly to the Level-3 products produced by the MODIS ocean and

land discipline groups. The monthly product provides a summary of the daily products obtained over a calendar month.

While there is no separation of the cloud parameters by ascending or descending node, there is a day/night separation and a process/no process decision for a number of parameters. Cloud fraction (from the cloud mask) and cloud top properties (i.e., cloud pressure and IR phase) are processed for both day and night and are provided in the Level-3 products as daytime only, nighttime only, and combined day and night. Cloud optical and microphysical properties are summarized for daytime only since they are not derived at night. The cloud fraction derived from the cloud mask is currently provided in the SDS name "Cloud_Fraction_IR". A daytime-only cloud fraction is derived also from successful optical and microphysical retrievals and aggregated by cloud thermodynamic phase. As an example, the SDS name for the liquid phase cloud fraction is "Cloud_Fraction_Water" (Platnick et al. 2003).

An example of the Level-3 monthly product is shown in Figure 5.4 for liquid water clouds from MODIS Terra in April 2003. Cloud optical thickness is shown in the top image and effective particle radius in the bottom image. These particular aggregation statistics are weighted by the quality assurance (QA) assignments given to each retrieved pixel. Unweighted statistics are also reported in the Level-3 file. Water cloud optical thicknesses are seen to be larger in the midlatitudes and poleward; especially noticeable are the large values throughout the southern oceans. Effective radius retrievals are seen to be generally smaller over the continents. Few results are shown for Antarctica at this time of year because the retrievals are performed only for daytime observations.

The Level-3 products also include histograms of cloud parameters and joint histograms derived from comparison of two parameters. Approximately 13 joint histograms are derived from the MOD06 cloud product. Note that the histogram counts are not weighted by the retrieval QA. Ten joint histograms are aggregated by cloud phase (5 for liquid water clouds and 5 for ice clouds). The joint histograms are computed from the following list: cloud optical thickness, effective particle radius, cloud-top temperature, and effective cloud amount. The other three joint histograms are aggregated by solar illumination (day, night, or combined day and night) and are built from cloud-top pressure and effective cloud amount. Examples of joint histograms for Terra and Aqua are shown in Figure 5.5. These examples are derived from data collected in August, 2003, between 10°-20° S, 70°-85° W (Peru/Humboldt Current regime), and shows the joint histogram of liquid water cloud optical thickness and effective particle radius. The Level-3 product bin sizes are used to form

the joint histogram. Further Level-3 algorithm and aggregation details, along with example images, can be found in King et al. (2003).

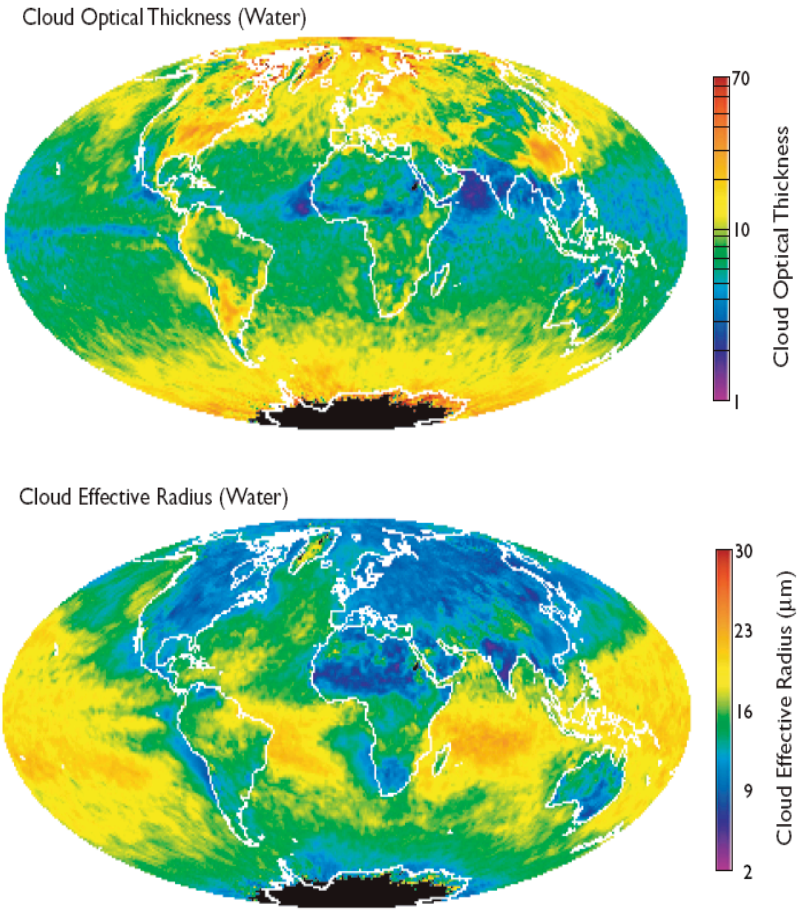

Fig. 5.4. MODIS Terra Level-3 April 2003 monthly aggregations for liquid water cloud retrievals of optical thickness (top) and effective particle radius (bottom)

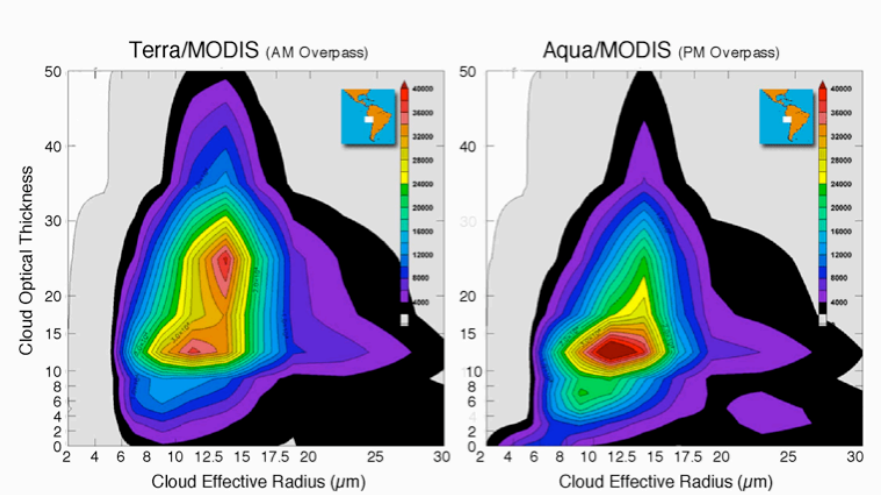

Fig. 5.5. Joint histogram of liquid water cloud optical thickness and effective particle size from products derived in August 2001, between 10°-20° S, 70°-85° W (coastal Peru/Chile)

5.5 Future Algorithm Efforts

A number of algorithm refinement and research efforts are currently being pursued. In this section we describe a few of these activities.

5.5.1 Detection of Multilayered Clouds

Satellite-based cloud property retrievals are performed under the assumption that observations for a given field of view contain a single cloud layer. The retrieved cloud top properties will contain the least error if the uppermost cloud layer is optically thick (i.e. opaque). However, observations indicate that multilayered clouds are common, especially for the case in which semi-transparent ice cloud overlies lower-level water clouds. In this situation, the assumption of a single cloud layer results in a cloud top pressure that lies between that of the upper and lower cloud layers. Error in the cloud top pressure propagates into errors in the inferred optical and microphysical properties.

New research is being conducted to determine when cirrus overlies water clouds in daytime and nighttime conditions (Baum et al. 2003; Nasiri and Baum 2004). While many approaches are being developed and tested, the daytime algorithm described here is based on SWIR bands at

1.6/2.1 and 11 μm, respectively. As noted previously in the discussion on cloud phase, ice particles absorb more radiation than water particles at the SWIR wavelengths (1.6/2.1 μm). Ice clouds also tend to reside at much higher altitudes than water clouds. The specific assumptions invoked for each pixel array (nominally 200 *x* 200 pixels) are that (a) at most two distinct cloud layers are present, (b) any pixels not uniquely associated with either of the two distinct cloud layers are classified as being multilayered, (c) clouds of both ice and water phase are present, (d) knowledge of the clear-sky SWIR/IR properties are known, and (e) a distance of at least 2 km in height between the layers is required to identify the separate layers.

The MOD35 cloud mask product provides information regarding clear and cloudy pixels, and cloud thermodynamic phase is assessed using the 8.5 μm and 11 μm brightness temperatures. Although either the 1.6- or 2.1-μm reflectance bands can be used in the multilayered cloud detection technique, the 2.1-μm band is used for the Aqua data because a number of the 1.6-μm band detectors on the Aqua MODIS instrument are inoperative (the band is comprised of 20 total detectors). To provide a confidence level for the assessment of whether a pixel contains more than one cloud layer, the method is applied as the pixel array, or tile, is moved gradually across the data granule, thereby testing each pixel (away from the granule borders) multiple times. The more times a pixel is flagged as containing multiple cloud layers, the higher the confidence in that assessment.

5.5.2 Improved Ice Cloud Microphysical and Optical Models

One major difference between midlatitude and tropical cirrus is that the tropical cirrus formed near centers of deep convection in mesoscale systems tend to contain more particles of larger size than the synoptically-generated cirrus in the midlatitudes. For most synoptically-generated midlatitude cirrus, the largest particle sizes measured are generally less than 800 μm. Larger particles tend to settle out quickly due to the relatively low updraft velocities in the cloud layer. Updraft velocities tend to be much higher in mesoscale systems associated with the generation of tropical cirrus. *In situ* measurements show that, in addition to high quantities of small particles, many large particles (greater than 1 cm in diameter) are also present even in the uppermost regions of the tropical anvil cirrus (Heymsfield et al. 2002).

Research is continuing towards the development of bulk scattering properties over a wider range of particle habit and size distributions (Yang et al. 2001, 2003: Heymsfield et al. 2002, 2003; Nasiri et al. 2002), which

will in turn expand the bulk scattering model libraries used for cloud remote sensing efforts. Scattering properties are now available for a much larger set of ice particles and include droxtals, hexagonal plates, solid columns, hollow columns, aggregates, and two- and three-dimensional bullet rosettes. Research is also underway to perform scattering calculations for more realistic large polycrystals such as those found in tropical cirrus.

5.5.3 Improved Land Spectral Albedo Maps

As discussed, the optical and microphysical retrieval algorithm requires surface albedo in visible and SWIR bands as the boundary condition for cloud radiative transfer modeling over land. Previously, a single 16-day composite of spectral albedo from the operational MOD43 product was available, requiring questionable assumptions on seasonal changes. A year's worth of MOD43 16-day spectral albedo composites have been archived in the GES DAAC since the last major optical and microphysical algorithm software delivery. With these data, a complete annual surface spectral albedo map is now available for use in the next production collection. Seasonality is built into the annual albedo maps. Cloud and seasonal snow cover, however, curtail retrievals to approximately half the global land surfaces on an annual equal-angle basis, precluding MOD43 albedo products from direct assimilation into the optical and microphysical production environment.

A temporal interpolation technique has been developed to fill missing data in the operational albedo product by imposing pixel-level and local regional ecosystem-dependent phenological behavior onto retrieved pixel temporal data in such a way as to maintain pixel-level spatial and spectral detail (Moody et al. 2005). The resulting value-added product provides spatially complete surface albedo maps and statistics for both direct and diffuse illuminations. Data are stored on one-minute and coarser resolution equal-angle grids for the first seven MODIS wavelengths (0.47 μm through 2.1 μm) and for three broadband wavelengths (0.3-0.7 μm, 0.3-5.0 μm and 0.7-5.0 μm).

5.5.4 Clear-sky Radiance Maps

An effort is being made to understand and mitigate differences between calculated and measured clear-sky infrared radiances to avoid modest cloud-top pressure assignment errors. These radiance differences can lead

to errors in retrieved cloud pressures (Wielicki and Coakley 1981). The primary cause of errors in the calculated clear-sky radiance is in the assignment of surface temperature from the gridded meteorological product, especially over land. The difficulty in assigning a realistic surface temperature over land is not unexpected given the range of diurnal variation, especially in areas of sparse vegetation.

Both daily and 8-day mean differences between observed and calculated clear-sky radiances will be generated for all MODIS mid- and long-wave infrared bands beginning with the MODIS Collection 5 processing. An example of 8-day mean biases (April 1-8, 2003) generated for Terra bands 31 and 34 is shown in Fig. 5.6. Clear-sky pixels (1-km resolution) are determined from cloud mask output (MOD35). Calculated radiances are derived from the 101-level Pressure-Layer Fast Algorithm for Atmospheric Transmittance (PFAAST; Strow et al. 2003). Application of the PFAAST requires temperature, moisture, and ozone profiles. The GDAS gridded product provides the temperature and moisture profiles while climatologically-averaged profiles of ozone are used. Biases will be accumulated on a global 25-km equal area grid.

5.6 Summary

This chapter provides a brief overview of the pixel-level (Level-2) and gridded (Level-3) MODIS operational cloud products. The core operational cloud products include cloud top pressure, thermodynamic phase, optical thickness, effective particle radius, and water path. These products are derived globally at spatial resolutions of either 1- or 5-km. Algorithm descriptions and data presented in sections 5.3 and 5.4 are applicable to the MODIS Atmosphere Team Collection 4 processing stream. The efforts described in section 5.5 were written before software was finalized for the Collection 5 processing stream that begun in April 2006 and therefore may not accurately represent the final operational algorithm status (e.g., multilayer cloud detection algorithm), nor should the section be considered a complete summary of all Collection 5 changes and updates. Further information including documentation, algorithm details and history, and quicklook imagery can be found at the MODIS atmosphere team web site: *http://modis-atmos.gsfc.nasa.gov*.

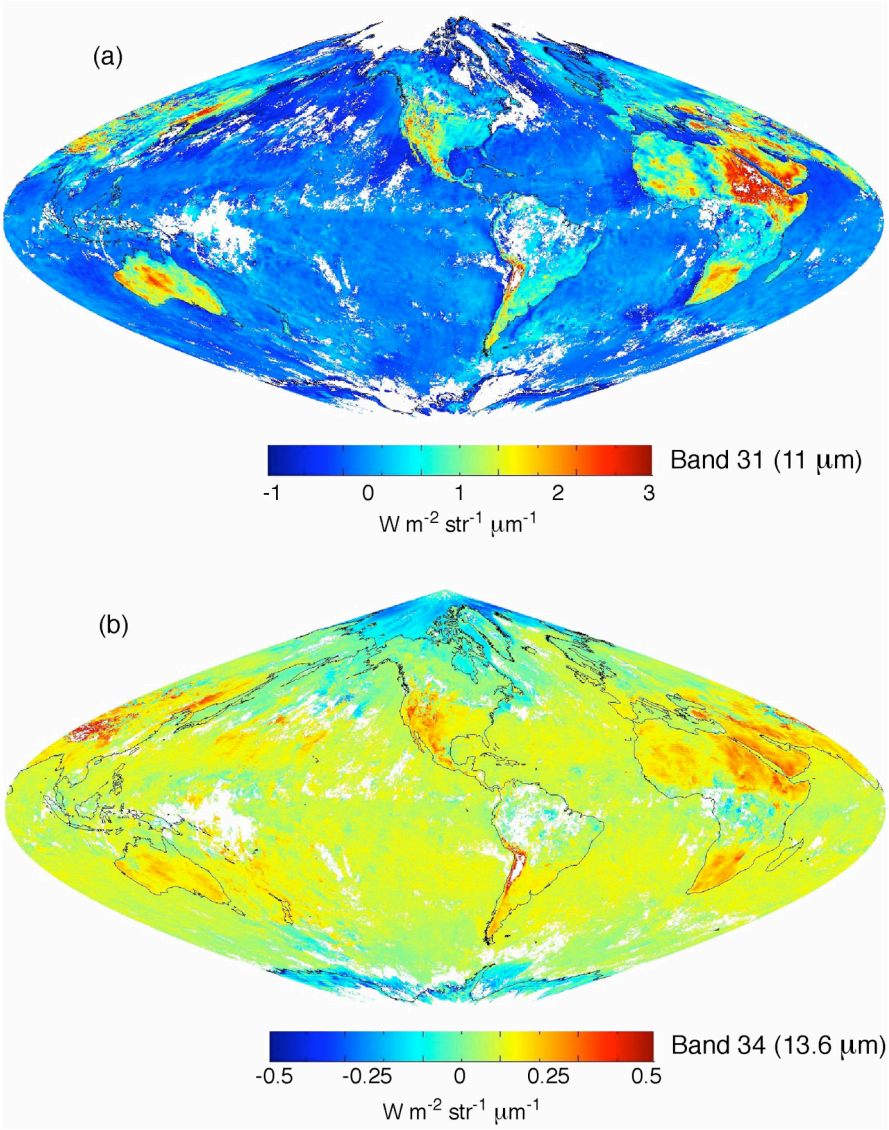

Fig. 5.6 Two examples of mean daytime Terra 8-day biases are shown: (a) 11 μm (band 31) and (b) 13.6 μm (band 34). Notice that in the band 31 example, large differences occur over land surfaces where diurnal heating is not adequately captured by input surface temperatures. The band 34 example indicates that perhaps upper tropospheric temperatures or tropopause locations were not accurate in this time period (April 1-8, 2003). Figures depict observed minus calculated radiances

References

Ackerman SA, Strabala KI, Menzel WP, Frey, RE, Moeller CC, Gumley LE (1998) Discriminating clear sky from clouds with MODIS. J Geophys Res 103:32141-32157

Baum BA, Kratz DP, Yang P, Ou S, Hu YX, Soulen PF, Tsay SC (2000a) Remote sensing of cloud properties using MODIS Airborne Simulator imagery during SUCCESS. I. Data and models. J Geophys Res 105:11767-11780

Baum BA, Soulen PF, Strabala KI, King MD, Ackerman SA, Menzel WP, Yang, P (2000b) Remote sensing of cloud properties using MODIS Airborne Simulator imagery during SUCCESS. II. Cloud thermodynamic phase. J Geophys Res 105:11781-11792

Baum BA, Frey RA, Mace GG, Harkey MK, Yang P (2003) Nighttime multilayered cloud detection using MODIS and ARM data. J Appl Meteor 42:905-919

Derber JC, Parrish DF, Lord SJ (1991) The new global operational analysis system at the National Meteorological Center. Weather Forecasting 6:538-547

Gao BC, Yang P, Han W, Li RR, Wiscombe WJ (2002) An algorithm using visible and 1.38 μm channels to retrieve cirrus cloud reflectances from aircraft and satellite data. IEEE Trans Geosci Remote Sens 40:1659-1668

Heymsfield AJ, Bansemer A, Field PR, Durden SL, Stith JL, Dye JE, Hall W, Grainger CA (2002) Observations and parameterizations of particle size distributions in deep tropical cirrus and stratiform precipitating clouds: Results from in situ observations in TRMM field campaigns. J Atmos Sci 59:3457-3491

Heymsfield AJ, Matrosov S, Baum BA (2003) Ice water path-optical depth relationships for cirrus and deep stratiform ice cloud layers. J Appl Meteor 42:1369-1390

King MD, Menzel WP, Kaufman YJ, Tanré D, Gao BC, Platnick S, Ackerman SA, Remer LA, Pincus R, Hubanks PA (2003) Cloud, Aerosol and Water Vapor Properties from MODIS. IEEE Trans Geosci Remote Sens 41:442-458

King MD, Platnick S, Yang P, Arnold GT, Gray MA, Riédi JC, Ackerman SA, Liou KN (2004) Remote sensing of liquid water and ice cloud optical thickness, and effective radius in the arctic: Application of airborne multispectral MAS data. J Atmos Oceanic Technol 21:857-875

Menzel WP, Wylie DP, Strabala KI (1992) Seasonal and diurnal changes in cirrus clouds as seen in four years of observations with the VAS. J Appl Meteor 31:370-385

Menzel WP, Purdom JFW (1994) Introducing GOES-I: The first of a new generation of Geostationary Operational environmental Satellites. Bull Amer Meteor Soc Vol 75 No 5: 757-781

Moeller CC, Revercomb HE, Ackerman SA, Menzel WP, Knuteson RO (2003) Evaluation of MODIS thermal IR band L1B radiances during SAFARI 2000. J Geophys Res 108:D13:8494

Moody EG, King MD, Platnick S, Schaaf CB, Gao F (2005) Spatially complete surface albedo data sets: Value-added products derived from Terra MODIS land products. IEEE Trans Geosci Remote Sens 43:144-158

Nasiri SL, Baum BA, Heymsfield AJ, Yang P, Poellot M, Kratz DP, Hu YX (2002) Development of midlatitude cirrus models for MODIS using FIRE-I, FIRE-II, and ARM *in-situ* data. J Appl Meteor 41:197-217

Nasiri SL, Baum BA (2004) Daytime multilayered cloud detection using multispectral imager data. J Atmos Oceanic Tech 21:1145-1155

Platnick S, King MD, Ackerman, SA, Menzel WP, Baum BA, Riédi JC, Frey RA (2003) The MODIS cloud products: algorithms and examples from Terra. IEEE Trans Geosci Remote Sens 41:459-473

Reynolds WR, Smith TM (1994) Improved global sea surface temperature analyses using optimum interpolation. J Climate 7:929-948

Strabala KI, Ackerman SA, Menzel WP (1994) Cloud properties inferred from 8-12 μm data. J Appl Meteorol 2:212-229

Strow L, Hannon S, Machado S, Motteler H, Tobin D (2003) An overview of the AIRS radiative transfer model. IEEE Trans Geosci Remote Sens 41:303-313

Wielicki, BA, Coakley JA (1981) Cloud retrieval using infrared sounder data: Error analysis. J Appl Meteorol 20:157-169

Wylie DP, Menzel WP (1999) Eight years of global high cloud statistics using HIRS. J Climate 12:170-184

Yang P, Gao BC, Baum BA, Wiscombe W, Hu YX, Nasiri SL, Heymsfield A, McFarquhar G, Miloshevich L (2001) Sensitivity of cirrus bidirectional reflectance to vertical inhomogeneity of ice crystal habits and size distributions. J Geophys Res 106:17267-17291

Yang P, Baum BA, Heymsfield AJ, Hu YX, Huang HL, Tsay SC, Ackerman S (2003) Single scattering properties of droxtals. J Quant Spectrosc Radiant Transfer 79-80:1159-1169